Supercurrents through gated superconductor–normal-metal–superconductor contacts: The Josephson transistor

Daniel D. Kuhn,[1] Nikolai M. Chtchelkatchev,[2] Gordey B. Lesovik,[2] and Gianni Blatter[1]
[1]*Theoretische Physik, ETH-Hönggerberg, CH-8093 Zürich, Switzerland*
[2]*L. D. Landau Institute for Theoretical Physics, 117940 Moscow, Russia*
(Received 30 June 2000; published 16 January 2001)

We analyze the transport through a narrow ballistic superconductor–normal-metal–superconductor Josephson contact with nonideal transmission at the superconductor–normal-metal interfaces, e.g., due to insulating layers, effective mass steps, or band misfits (SIN interfaces). The electronic spectrum in the normal wire is determined through the combination of Andreev reflection and normal reflection at the SIN interfaces. Strong normal scattering at the SIN interfaces introduces electron- and holelike resonances in the normal region that show up in the quasiparticle spectrum. These resonances have strong implications for the critical supercurrent I_c that we find to be determined by the lowest quasiparticle level: tuning the potential μ_{x0} to the points where electron- and holelike resonances cross, we find sharp peaks in I_c, resulting in a transistor effect. We compare the performance of this resonant Josephson-transistor with that of a superconducting single electron transistor.

DOI: 10.1103/PhysRevB.63.054520 PACS number(s): 74.80.Fp, 74.50.+r, 74.60.Jg

I. INTRODUCTION

The ability to control the supercurrent flow through narrow superconductor–normal-metal–superconductor (SNS) contacts is not only of scientific interest but also provides many opportunities for applications.[1] With recent progress in nanofabrication technology it has become possible to study devices in which electrons propagate ballistically and where the transport proceeds via few conduction channels.[2] Using gated SNS junctions,[3] the transparency of the normal region can be manipulated: in a transparent wire, Andreev scattering at the NS boundaries produces phase-sensitive quasiparticle levels that carry large supercurrents; conversely, if the transmission is not ideal, the admixture of normal scattering reduces the supercurrent transport. Accordingly, SNS junctions with a tunable transmission through the normal part define a natural setup for a superconducting transistor device.[4–6]

Recent interest on transport through narrow channels and quantum point contacts concentrates on diverse phenomena such as conductance quantization in normal constrictions,[2,7–10] supercurrent quantization in superconducting SNS junctions,[3,8,11–13] or the transistor effect in superlinks using either gated structures[4,6,14] or injection techniques.[15–17] Experimentally, such junctions are fabricated using superconductor–semiconductor heterostructures,[2,3,14,16] break junctions,[7–9] metal nanolithography,[15,17] or with the use of carbon nanotubes.[18] Theoretically, transport through normal constrictions has been studied by Glazman *et al.*[10,19] within a quasiclassical description assuming adiabatic joints between the channel and the leads. The corresponding extension to superconducting leads by means of a scattering matrix approach is due to Beenakker,[11] see also Ref. 20, while Furusaki *et al.*[12] proceeded with the numerical analysis of junctions with nonadiabatic geometries and nonideal interfaces. The evolution of the quasiparticle spectrum and the supercurrent quantization in a gated narrow SNS junction, as well as its transformation into a SIS tunnel junction, has been recently described by Chtchelkatchev *et al.*[13] Here, we extend this analysis to the study of SINIS junctions, where I stands for a nonideal interface between the superconducting banks S and the normal channel N.

In an ideal SNS junction[21] the quasiparticle spectrum is determined by the Andreev scattering[22] at the SN boundaries producing phase-sensitive levels transporting large supercurrents.[13] The position and relative arrangement of these states strongly depends on the chemical potential in the wire as well as on the phase difference between the superconducting banks. The inclusion of weak normal scattering at the SIN interface will only softly modify this quasiparticle spectrum through the mixing of (left and right) current-carrying Andreev states. On the contrary, strong interface scattering introduces electron- and holelike resonances within the normal region, defining a new starting point. The position of these resonances again depends on the wire's effective chemical potential. Tuning a pair of electron- and holelike resonances to degeneracy, these will be mixed by the Andreev scattering, and new phase-sensitive levels are formed carrying supercurrent. This mechanism then provides a natural setup for the implementation of a superconducting Josephson field effect transistor,[4,6] where the supercurrent is switched on and off by tuning the scattering resonances into degeneracy through the manipulation of a potential, e.g., through external gates. Model studies of such systems for individual resonances have been carried out recently by Wendin *et al.*[6]

Below we proceed in two steps: After a brief definition of the problem (Sec. II), we first determine the scattering states of the corresponding problem where the superconducting banks are replaced by normal-metallic leads, the NININ junction. Second, we reinstall the superconducting banks and determine the mixing of the (electron- and holelike) normal scattering states through Andreev scattering at the normal-superconductor interface. In Sec. III we analyze the quasiparticle spectrum for weak and strong normal scattering at the NIS interfaces. Section IV is devoted to the calculation of the supercurrent; we discuss the functionality of the resonant Josephson transitor (RJT) and compare this device with the superconducting single electron transistor (SSET).

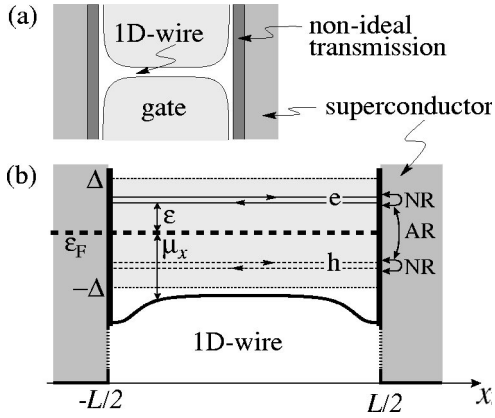

FIG. 1. Narrow channel SINIS contact with nonideal interfaces, e.g., insulating layers, effective mass steps, or band misfits. We consider adiabatic constrictions to avoid the mixing of transverse channels. (a) Geometrical setup showing the gates narrowing the wire, (b) potential landscape with a flat barrier bounded by δ scatterers modeling insulating layers. All sources of nonideal transmission account for *normal* reflections (NR), whereas the discontinuities of the gap parameter Δ are responsible for Andreev reflections (AR).

II. BALLISTIC CONTACTS: SCATTERING MATRIX APPROACH

We consider a narrow metallic lead with few transverse channels connecting two superconducting banks with a rectangular pair potential $\hat{\Delta}(x<-L/2)=\Delta\exp(i\varphi_L)$, $\hat{\Delta}(|x|<L/2)=0$, and $\hat{\Delta}(x>L/2)=\Delta\exp(i\varphi_R)$, see Fig. 1(a). Joining the channel adiabatically to the superconducting banks, the transverse channels in the wire are separable[19] and for each of them the quasiparticle spectrum ε_ν is determined through the one-dimensional (1D) Bogoliubov-de Gennes equation (we choose states with $\varepsilon_\nu\geqslant 0$)

$$\begin{bmatrix} \mathcal{H}_0 & \hat{\Delta}(x) \\ \hat{\Delta}^*(x) & -\mathcal{H}_0 \end{bmatrix}\begin{bmatrix} u_\nu(x) \\ v_\nu(x) \end{bmatrix}=\varepsilon_\nu\begin{bmatrix} u_\nu(x) \\ v_\nu(x) \end{bmatrix}, \tag{1}$$

with $\mathcal{H}_0=-\hbar^2\partial_x[1/2m(x)]\partial_x+U(x)-\mu_x(x)$ and where u_ν and v_ν denote the electron- and holelike components of the wave function Ψ_ν. The potential $U(x)$ induces normal scattering at the NS interface and is due to an insulating layer or a band offset, for example. Similarly, the mass $m(x)$ may change at the NS interface, again generating normal scattering. The transverse energy $\varepsilon_\perp(x)$ of the channel is enclosed in the effective chemical potential[19] $\mu_x(x)=\varepsilon_F-\varepsilon_\perp(x)$. We will also make use of the kinetic energies $E=\varepsilon_F\pm\varepsilon$ of electron $(+)$ and hole $(-)$ states as measured with respect to the band bottom in the superconductors.

The spectrum splits into continuous and discrete contributions and we will concentrate on the latter part with $\varepsilon_\nu<\Delta$ in the following, as it provides the main contribution to the critical supercurrent in the most interesting transport regimes, see below. We solve the Bogoliubov-de Gennes equation for the SINIS junction with the help of the usual transfer-matrix technique.[23] In order to do so we first have to determine the resonance structure of the related NININ problem that arises if we replace the superconductors by normal metallic leads.

A. NININ junctions

We expand the scattering states in a basis of in- and outgoing states $\Psi_{R,L}^{\text{in,out}}$ on both sides of the wire, with phases that vanish at the interfaces[24] $\pm L/2$,

$$\Psi_L(x)=a_L^{\text{in}}e^{ik(x+L/2)}+a_L^{\text{out}}e^{-ik(x+L/2)}, \tag{2}$$

$$\Psi_R(x)=a_R^{\text{in}}e^{-ik(x-L/2)}+a_R^{\text{out}}e^{ik(x-L/2)}, \tag{3}$$

with $k(E)=\sqrt{2mE}/\hbar$ the wave vector of an incident particle. The energy-dependent scattering matrix $\mathcal{S}$ connects the expansion coefficients $a_{R,L}^{\text{in,out}}$ (here, t and r denote the moduli of the matrix elements),

$$\begin{bmatrix} a_R^{\text{out}} \\ a_L^{\text{out}} \end{bmatrix}=\begin{bmatrix} t\exp(i\chi^t) & -r\exp(i[2\chi^t-\chi^r]) \\ r\exp(i\chi^r) & t\exp(i\chi^t) \end{bmatrix}\begin{bmatrix} a_L^{\text{in}} \\ a_R^{\text{in}} \end{bmatrix}; \tag{4}$$

with this definition of the $\mathcal{S}$ matrix and the basis states, the scattering phases account for the propagation through the wire; e.g., for a vanishing transverse energy in the normal region and in the absence of any interface barrier a finite phase $\chi^t=kL$ is picked up.

We describe the effective chemical potential in the normal region through a smooth function characterized by its minimum $\mu_x(0)=\mu_{x0}$ and a positive curvature $m\Omega^2=\partial_x^2\mu_x$ [see Fig. 1(b)]. The parameter μ_{x0} (i.e., the diameter of the metallic wire) is assumed to be tunable by means of external electrostatic gates. In a long wire the potential is flat, $\hbar\Omega\ll\Delta$, and produces a sharp switching between transmission and reflection within the energy interval $\hbar\Omega$; the corresponding transverse energy $\varepsilon_\perp(x)$ defines a smooth and flat potential barrier in the interval $(-L/2,\ L/2)$. In the following we refer to such barriers as *smooth* and $t_i\exp(i\chi^{t_i})$ and $r_i\exp(i\chi^{r_i})$ denote the associated ''inner'' scattering amplitudes describing the motion of the quasiparticles between $-L/2+0$ and $L/2-0$ [we use an analoguous definition of the inner scattering amplitudes as in Eq. (4)]. The particular smooth geometry of such inner barriers justifies the application of the Kemble formula[10] for the transmission probability, $t_{i\pm}^2=1/\{1+\exp[-2\pi(\mu_x(0)\pm\varepsilon)/\hbar\Omega]\}$, whereas the quasiclassic method can be used to determine the scattering phases χ^{t_i} and χ^{r_i}.

In order to obtain the global scattering amplitudes $t\exp(i\chi^t)$ and $r\exp(i\chi^r)$ of the junction we have to include effects of normal scattering at the boundaries. As a typical example we consider symmetric smooth barriers of height $\varepsilon_F-\mu_{x0}$ bounded by Dirac scatterers of strength V_0 at the interfaces (such a setup describes an NININ junction with insulating layers at the interfaces; see the Appendix for a brief discussion of other typical cases).

First, we concentrate on the global *transmission* amplitude $t\exp(i\chi^t)$, which is easily expressed in terms of the scattering amplitudes of the inner barrier and the Dirac δ scatterers; see the Appendix for details of the calculation. The

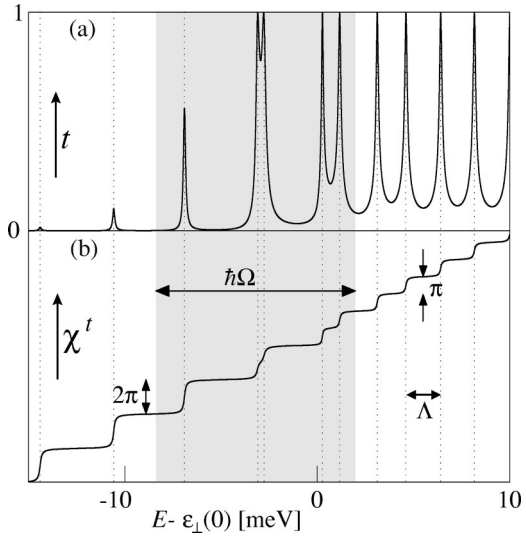

FIG. 2. Modulus and phase of the transmission amplitude through a parabolic barrier with δ scatterers at the edges (parameters: $Z=2$, $\varepsilon_\perp(0)=5$ eV, $L=2500$ nm). Note that the energy E is swept and $\varepsilon_\perp(0)$ is kept fixed. A similar resonance structure is found for other sources of nonideal transmission at $\pm L/2$.

main effect of the scattering at the channel boundaries is to introduce resonances at energies $E_{\rm res}$, which we call *perfect* (*imperfect*) if $t(E_{\rm res})=1$ (<1). For energies $E>\varepsilon_\perp(0)+\hbar\Omega/2$ the electrons easily propagate through the channel, while the reflection at the boundaries produces almost equidistant resonances with a spacing $\Lambda\approx\pi/\partial_E\chi^{t_i}\sim 2(\mu_{x0}\varepsilon_{\rm L})^{1/2}$, with $\varepsilon_{\rm L}=\hbar^2\pi^2/2mL^2$ (see Fig. 2; the last relation describes the case of a flat inner barrier). On the contrary, for small energies below $\varepsilon_\perp(0)-\hbar\Omega/2$, tunneling suppresses the propagation through the channel and only imperfect resonances separated by $\sim 2\Lambda$ survive. In the intermediate region, pairs of perfect resonances collapse and become imperfect. Moreover, the scattering phase χ^t grows with the energy and picks up a phase of π and 2π at perfect and imperfect resonances, respectively. We refer to resonances at energies $E_{\rm res}=\varepsilon_F+\hat{\varepsilon}_{\rm res}$ above ε_F as *electronic* and to those below, at $E_{\rm res}=\varepsilon_F-\check{\varepsilon}_{\rm res}$, as *holelike* resonances. Below, we will be mostly concentrating on the propagating regime with $E>\varepsilon_\perp(0)+\hbar\Omega/2$. In this regime the global transmission amplitude takes the form $(t_{i\pm}\approx 1)$

$$t\exp(i\chi^t)=\frac{e^{i\chi^{t_i}}}{1-Z^2+i2Z+Z^2e^{i2\chi^{t_i}}}, \tag{5}$$

with $Z=mV_0/\hbar^2k_F$ the dimensionless parameter giving the strength of the scattering potential. Resonances of width

$$\Gamma=\frac{2}{\partial_E\chi^t}=\frac{2\Lambda}{\pi}\frac{T}{2-T},\quad \text{with}\quad \Lambda=\frac{\pi}{\partial_E\chi^{t_i}} \tag{6}$$

and a transmission probability $T=1/(1+Z^2)$ appear as the denominator in Eq. (5) touches the complex unit circle (note that $\Gamma\to 2\hbar v/L$, with v the particle velocity, in the absence of any scattering potential).

For symmetric barriers the *reflection* amplitude $r\exp(i\chi^r)$ is determined (up to ± 1) by the unitarity of the scattering matrix, i.e., $r=(1-t^2)^{1/2}$ and $\chi^r=\chi^t+\pi(n+1/2)$. The integer n jumps by unity at perfect resonances.

B. SINIS junctions

After evaluating the normal scattering amplitudes we can reinstall the superconductors and match the scattering states in the normal region with the evanescent modes in the superconducting banks. We make use of the Andreev approximation[22] and obtain the quantization condition[13] (see also Refs. 11 and 25)

$$\cos(\chi_+^t-\chi_-^t-\alpha)=r_+r_-\cos\beta+t_+t_-\cos\varphi, \tag{7}$$

where the $+(-)$ signs refer to the kinetic energies $\varepsilon_F\pm\varepsilon$ of the electron(hole)like states.[26] The Andreev scattering at the NS boundaries introduces the phase $\alpha=2\arccos(\varepsilon/\Delta)$ decreasing from π at $\varepsilon=0$ to 0 at the gap $\varepsilon=\Delta$, as well as the phase difference $\varphi=\varphi_L-\varphi_R$ between the two superconducting banks. For symmetric barriers the phase $\beta=(\chi_+^t-\chi_+^r)-(\chi_-^t-\chi_-^r)$ is a multiple of π and produces a smooth function $r_+r_-\cos\beta$ changing sign at perfect resonances [see Fig. 5(b)].

The case of an ideal SNS junction where the effective chemical potential joins smoothly to the band bottom in the superconductors has been analyzed by Chtchelkatchev *et al.*[13] In this special situation the global and inner scattering amplitudes coincide and resonances are absent. Sweeping μ_{x0}, they find a one parametric (μ_{x0}) family of discrete spectra describing the transition of an insulating SIS tunnel junction (at $\mu_{x0}\ll-\Delta$) into a ballistic SNS structure (at $\mu_{x0}\gg\Delta$), see Fig. 3(a). More precisely, electronic levels with an exponentially small dependence on the phase φ are converted into phase sensitive Andreev levels as μ_{x0} is increased, i.e., as the band bottom in the wire is lowered. It turns out that the critical supercurrent is carried by the lowest state, $I_c=\max_\varphi[(2e/\hbar)\partial_\varphi\varepsilon_0]$, and is realized for a phase $\varphi=\pi-0$. Increasing the channel width, the critical supercurrent increases in steps of $e/(\tau_0+\hbar/\Delta)$ as new transverse channels open. The travel time τ_0 of the quasiparticles is easily calculated within the quasiclassical scheme and approaches the asymptotic value $\tau_0\sim L/v_{F,x}$ in the open channel. This analysis explains the dependence of the nonuniversal critical supercurrent steps on the junction parameters.

In the following we go beyond the analysis of Chtchelkatchev *et al.* and determine the spectrum and the supercurrent transport in a narrow ballistic SINIS Josephson junction including resonant barriers in the normal region, see Fig. 1(b).

III. QUASIPARTICLE SPECTRUM

Below, we shall see that the bound-state spectrum of junctions with smooth barriers is only slightly modified by switching on weak resonances, see Fig. 3(b), with the degeneracy of the Andreev levels at $\varphi=0$ and π lifted. For a fixed pair of levels $\varepsilon^{(\pm)}$, this splitting $\delta\varepsilon=\varepsilon^{(+)}-\varepsilon^{(-)}$ is roughly a periodic function of μ_{x0} with a period Λ reflecting the

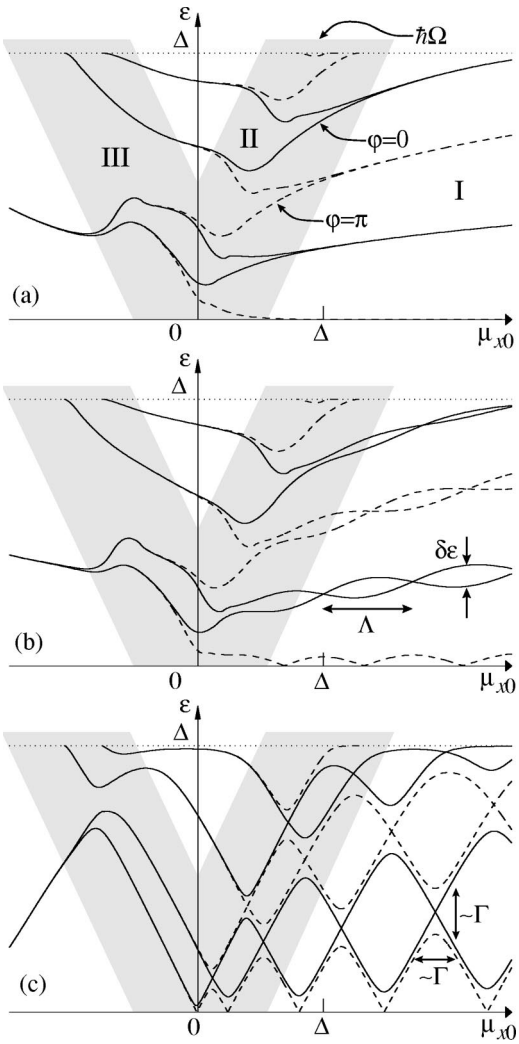

FIG. 3. Discrete energy spectrum for a smooth parabolic potential barrier bounded by Dirac scatterers of strength V_0 ($Z = mV_0/\hbar^2 k_F$; parameters are chosen to emphasize the overall structure of the spectrum). In regions I and II the quasiparticle energies depend on the phase φ ($\varphi=0$: solid lines, $\varphi=\pi$: dashed lines). Note that the degeneracies in region I are lifted for $\varphi \neq 0, \pm\pi$. (a) The unperturbed spectrum for $Z=0$ as discussed by Chthelkatchev *et al.*[13] (b) At $Z=0.1$ the junction exhibits weak resonances that lead to a splitting in the Andreev spectrum; the period Λ reflects the resonance spacing. (c) For $Z=1$ the junction develops distinct resonances to which the quasiparticle levels are pinned. The remaining degeneracies are a consequence of the almost identical resonance shapes.

resonance spacing. As the strength of the interface scattering increases the discrete spectrum is gradually distorted [see Fig. 3(c)]; the phase sensitivity at large chemical potential μ_{x0} (region I) is reduced and the bound-state energies align with the resonance energies of the normal NININ setup. The effect of interface scattering on the continuum part of the spectrum has been analyzed in Ref. 25.

A. Weak resonances

We first concentrate on weak resonances characterized by a small scattering parameter $Z \ll 1$. In particular, we aim at

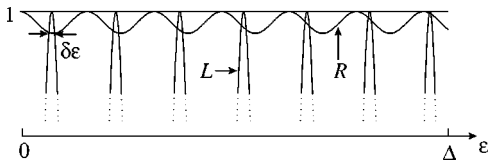

FIG. 4. The quasiparticle energies are determined by the intersections of the right- and the left-hand side (R and L) of the quantization condition (7). Every maximum in L contributes a pair of trapped levels split by $\delta\varepsilon$.

estimating the level splitting in the Andreev spectrum shown in Fig. 3(b). Using Eq. (5) we evaluate the terms on the right side of the quantization condition (7) to lowest order in Z and find $t_+t_- = 1-2Z^2[\cos^2\chi_+^{t_i} + \cos^2\chi_-^{t_i}]$ and $r_+r_- = 4Z^2|\cos\chi_+^{t_i}||\cos\chi_-^{t_i}|$. For symmetric barriers and as a consequence of the unitarity of the scattering matrix, the rescaled phase $\beta(\varepsilon)/\pi$ is an integer valued function starting from 0 at $\varepsilon=0$ and jumping by unity whenever ε lines up with a (perfect) resonance at $\hat{\varepsilon}_{\rm res}$ or $\check{\varepsilon}_{\rm res}$ of the junction. We then may write $\cos\beta=(-1)^n$, where $n(\varepsilon)$ denotes the number of perfect resonances within the interval $(0,\varepsilon)$. Hence, $\cos\beta$ generates a smooth contribution $r_+r_-\cos\beta = 4Z^2\cos\chi_+^{t_i}\cos\chi_-^{t_i}$, which is small, of order Z^2. Finally, the scattering phase $\delta\chi^t = \chi_+^t - \chi_-^t$ in Eq. (7) may be identified with $\delta\chi^{t_i} = \chi_+^{t_i} - \chi_-^{t_i}$; the deviation of $\delta\chi^t$ from $\delta\chi^{t_i}$ provides only small corrections of order Z^2 to the splitting in the Andreev spectrum and thus can be disregarded.

At $\varphi=0$ the right-hand side of Eq. (7) can be expressed as $R = 1-2Z^2(1-\cos\delta\chi^{t_i})(1-\cos\Sigma\chi^{t_i})$, while the left-hand side takes the form $L=\cos(\delta\chi^{t_i}-\alpha)$. The sum $\Sigma\chi^{t_i} = \chi_+^{t_i} + \chi_-^{t_i}$ of the scattering phases depends only weakly on ε but increases linearly in μ_{x0} with a slope $2\pi/\Lambda$, as follows from linearizing $\chi_\pm^{t_i}(\varepsilon,\mu_{x0})$. On the other hand, the phase difference $\delta\chi^{t_i}$ increases with energy ε but is roughly independent of μ_{x0}. Both terms L and R then show an oscillating dependence on $\delta\chi^{t_i}$ and on the energy ε (see Fig. 4), while their relative phase $\alpha(\varepsilon)$ slowly decreases from π at $\varepsilon=0$ to 0 at $\varepsilon=\Delta$. Thus, for small energies ($\varepsilon \ll \Delta$) the maxima in L coincide with the minima in R and we obtain a large splitting,

$$\delta\varepsilon \approx \frac{4}{\pi} Z\Lambda|\sin\chi_+^{t_i}|, \tag{8}$$

to lowest order in Z (with $\chi_+^{t_i}$ evaluated at $\varepsilon=0$). The corresponding splitting for $\varphi=\pm\pi$ is proportional to $|\cos\chi_+^{t_i}|$ with the same prefactor. With increasing energy the phases of L and R match up and the splitting becomes small; see Fig. 4. The monotonous decrease of the splitting is most prominent in long junctions with many trapped levels.

As manifested in Eq. (8) the splitting vanishes at specific degeneracy points: we define the (l,m) degeneracy via the condition $\varepsilon_F = (E_{\rm res}^l + E_{\rm res}^m)/2$, where l and m count the perfect resonances. This implies $|E_{\rm res}^l - E_{\rm res}^m|/2 = \hat{\varepsilon}_{\rm res} = \check{\varepsilon}_{\rm res} = \varepsilon_{\rm res}^d$. The ideal degeneracies in Eq. (8) originate from the

assumption that all perfect resonances have the same symmetric shape, $t(E^{l}_{\rm res}+\delta E)=t(E^{m}_{\rm res}\pm\delta E)$. For $\varphi=0$ $(\pm\pi)$ and for even (odd) values of $n(\varepsilon^{d}_{\rm res})$ the right-hand side of the quantization condition (multiplied by -1) equals unity, $r_+r_-+t_+t_-=r_+^2+t_+^2=1$, and thus the trapped levels appear in degenerate pairs. The degeneracy is lifted, if we take into account that the perfect resonances are not identical.

B. Strong resonances

Let us next study the effects of *strong* resonances. Without loss of generality we again discuss the symmetric barrier bounded by δ scatterers (see also Ref. 25). We concentrate on the open channels in region I [see Fig. 3(a)]; the other regimes in the (ε,μ_{x0}) plane are less interesting and we will briefly discuss them at the end. For sharp resonances with $\Gamma\ll\Delta$ the transmittivity close to a resonance $\varepsilon_{\rm res}$ assumes a Lorentz profile[27] $t_\pm(\varepsilon)=(\Gamma/2)/\sqrt{(\varepsilon-\varepsilon_{\rm res})^2+(\Gamma/2)^2}$ and the scattering phase takes the usual form $\chi^t_\pm(\varepsilon)=\chi^t(E_{\rm res})\pm\arctan[2(\varepsilon-\varepsilon_{\rm res})/\Gamma]$.

Figure 5 shows the terms entering the quantization condition (7). Particles incident from the left on the normal region are reflected back $(r_+\approx1)$ unless their energy coincides with an electronic resonance energy $[r_+(\hat{\varepsilon}_{\rm res})=0$ for perfect resonances]. Similarly, holes are only transmitted if their energy corresponds to a holelike resonance energy $[r_-(\check{\varepsilon}_{\rm res})=0]$. Consequently, the product r_+r_- remains close to unity but sharply drops to zero at perfect resonance energies [see Fig. 5(a)]. Similar to the case of weak resonances the product r_+r_- becomes a smooth function of ε when combined with $\cos\beta=(-1)^n$, see Fig. 5(b). Furthermore, the phase sensitive term $t_+t_-\cos\varphi$ vanishes practically over the entire interval $[0,\Delta]$ [see Fig. 5(c)] with the exception of specific points where particle- and hole resonances become *degenerate*, $\hat{\varepsilon}_{\rm res}=\check{\varepsilon}_{\rm res}=\varepsilon^{d}_{\rm res}$.

The left-hand side of Eq. (7) is mainly determined by the phase difference $\delta\chi^t$ exhibiting sharp steps by π at the resonance energies $\check{\varepsilon}_{\rm res}$ and $\hat{\varepsilon}_{\rm res}$, while remaining constant in between (in our discussion of the situation away from region I below, we will have to distinguish perfect from imperfect resonances, as the latter involve phase jumps by 2π). Hence, in the limit $\Gamma\to0$ we obtain $\cos(\delta\chi^t-\alpha)=(-1)^n\cos\alpha$, while a small finite value of Γ will smooth the discontinuities [see Fig. 5(d)]. All the terms entering the quantization condition (7) then are pronounced functions of ε near the resonance energies, while staying roughly constant everywhere else. As a consequence, the intersections of the left- and the right-hand side of Eq. (7) come to lie close to the resonance energies of the NININ junction, as shown in Fig. 5(e) and we conclude that the normal-state resonances attract the quasiparticle bound states, $\varepsilon\approx\varepsilon_{\rm res}$ to zeroth order in Γ. The predicate *electronic*- and *holelike* states then can be naturally assigned to the trapped levels in the SINIS junction, too.

In region I [see Fig. 3(a)], the bound-state energy close to an *isolated resonance* is determined by the implicit equation

$$\varepsilon=\varepsilon_{\rm res}-\frac{\Gamma}{2}\cot\,[\alpha(\varepsilon)/2]. \tag{9}$$

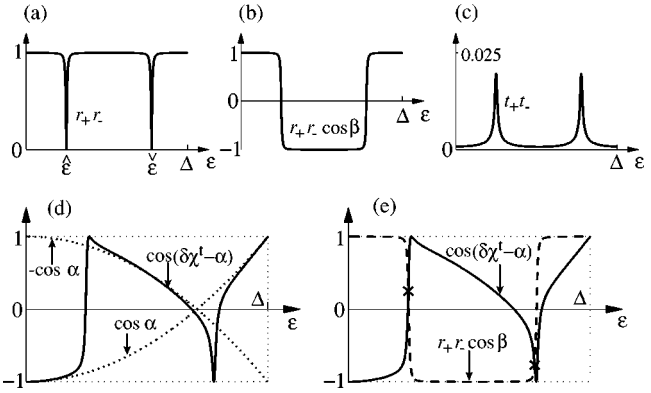

FIG. 5. The various terms entering the quantization condition (7) in the limit $\Gamma\ll\Delta$: We show the case of perfect *isolated* resonances $(|\hat{\varepsilon}-\check{\varepsilon}|\gg\Gamma)$, where the product t_+t_- is small at all energies (here, $t_+t_-<0.025$). The bound-state energies [marked with crosses in (e)] are determined by the intersections of $\cos(\delta\chi^t-\alpha)$ and $r_+r_-\cos\beta$.

This equation follows directly from the quantization condition (7), with $t_+\exp(i\chi^t_+)$ described by an ideal Lorentzian resonance while $t_-=0$, $r_-=1$, and $\chi^t_-=\chi^t_+(\varepsilon_{\rm res})+n(\varepsilon_{\rm res})\pi$ is constant (or vice versa $+\leftrightarrow-$). For $\varepsilon\ll\Delta$ we may approximate $\alpha(\varepsilon)\approx\pi$, while at $\varepsilon\lesssim\Delta$ Eq. (9) is easily analyzed graphically (note, however, that the above assumptions for $t_\pm$ and $\chi^t_\pm$ are only valid if $|\varepsilon-\varepsilon_{\rm res}|\ll\Delta$). The phase independence of the quasiparticle states in the presence of strong normal scattering is made explicit in the result (9).

Close to the *particle-hole degenerate resonances* the phase sensitive term $\propto t_+t_-=(\Gamma/2)^2/[(\varepsilon-\varepsilon^{d}_{\rm res})^2+(\Gamma/2)^2]$ is of order unity and we obtain pairs of trapped levels

$$\varepsilon^{(\pm)}=\begin{cases}\varepsilon^{d}_{\rm res}-\dfrac{\Gamma}{2}\left[\cot\left(\dfrac{\alpha}{2}\right)\pm\dfrac{|\sin(\varphi/2)|}{\sin(\alpha/2)}\right], & n(\varepsilon^{d}_{\rm res})\ \text{ even},\\[2ex] \varepsilon^{d}_{\rm res}-\dfrac{\Gamma}{2}\left[\cot\left(\dfrac{\alpha}{2}\right)\pm\dfrac{|\cos(\varphi/2)|}{\sin(\alpha/2)}\right], & n(\varepsilon^{d}_{\rm res})\ \text{ odd}\end{cases} \tag{10}$$

(we assume both scattering amplitudes $t_\pm\exp(i\chi^t_\pm)$ to be described by the same Lorentzian centered around $\varepsilon^{d}_{\rm res}$; Eq. (10) agrees with the result of Ref. 6 obtained for a short junction,[27] see also Ref. 25). The levels (10) are manifestly phase sensitive and become degenerate at $\varphi=0$ for even n and at $\varphi=\pi$ if n is odd. For low energies $\varepsilon\ll\Delta$ we estimate $\alpha(\varepsilon)\approx\pi$ and the maximum level splitting is $\delta\varepsilon\approx\Gamma$. We conclude that phase sensitivity survives only in a narrow interval of order $\Delta\mu_{x0}\sim\Gamma$ around the degeneracy points μ^{d}_{x0}, being negligible everywhere else [see Fig. 3(c)].

Above, we have found the trapped levels belonging to a branch $\varepsilon_{\rm res}(\mu_{x0})$ of perfect resonances at the degeneracy points μ^{d}_{x0} and far away, $|\mu_{x0}-\mu^{d}_{x0}|\gg\Gamma$. In between we can interpolate Eqs. (9) and (10) by means of the usual hyperbolic dispersion relation and obtain (in the limit $\varepsilon\ll\Delta$; $\alpha\approx\pi$)

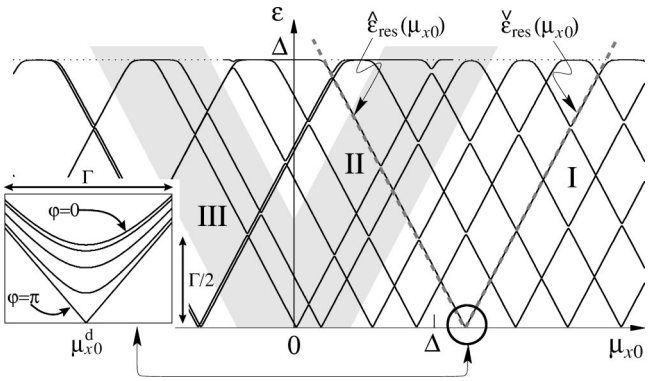

FIG. 6. Discrete spectrum for a triple barrier generating narrow resonances [from a numerical solution of the quantization condition (7)]. The levels are pinned to the resonances; note that holelike resonance energies $\check{\varepsilon}_{\rm res}$ grow with μ_{x0}, whereas electronic resonance energies $\hat{\varepsilon}_{\rm res}$ decrease. In region II (III) the holelike (electronic) levels pair up such that the branches of imperfect resonances carry two bound states. The inset shows the lowest level near the degeneracy point μ^d_{x0} for different values of φ ($\varphi = j\pi/4$, $j=0\ldots4$).

$$\varepsilon^{(\pm)}(\mu_{x0}) = \varepsilon^d_{\rm res} \pm \sqrt{(\mu_{x0}-\mu^d_{x0})^2 + [\Gamma\cos(\varphi/2)/2]^2}, \tag{11}$$

where we have assumed that $n(\varepsilon^d_{\rm res})$ is odd and $\partial_{\mu_{x0}}\check{\varepsilon}_{\rm res} \approx -\partial_{\mu_{x0}}\hat{\varepsilon}_{\rm res} \approx 1$. The result (11) will be useful in our discussion of the transport properties below.

In region II [see Fig. 3(a)] the perfect holelike resonances pair up and collapse as μ_{x0} is lowered, thus generating imperfect resonances, see Fig. 6. The analogous collapse of the electronic resonances is shifted to region III. Note that an imperfect resonance carries *two* nearly degenerate levels guaranteeing that the number of bound states remains conserved upon changing μ_{x0}.

C. Other sources of nonideal transmission

The above analysis has been based on δ scatterers modeling the effects of an insulating layer in an SIN interface. Assuming other sources of nonideal transmission at $\pm L/2$ we have to modify some of the above results: In order to describe junctions with potential steps V_S at the edges we introduce the wave vector $k_{\rm nw} = \sqrt{2m(E-V_S)}/\hbar$ in the normal wire and distinguish it from the analogous quantity $k_{\rm sc} = \sqrt{2mE}/\hbar$ in the superconductor. With $\kappa \equiv (k_{\rm sc}/k_{\rm nw} + k_{\rm nw}/k_{\rm sc})/2 \geqslant 1$, the transmission probability takes the form $T = 2/(1+\kappa)$ (see the Appendix). In the presence of weak resonances ($T \lesssim 1$), Eq. (8) for the gaps in the Andreev spectrum reads $\delta\varepsilon \approx 4\Lambda\sqrt{1-T}|\cos\chi^t_i|/\pi$, while the results for strong resonances remain the same [see Eq. (9)]. A step in the effective mass at the interface produces a similar result: with $m(|x|>L/2) = m_{\rm sc}$ and $m(|x|<L/2) = m_{\rm nw}$, the ratio of wave vectors entering the parameter κ takes the form $k_{\rm sc}/k_{\rm nw} = \sqrt{m_{\rm sc}/m_{\rm nw}}$. Finally, combining all three effects, a potential step, an effective mass discontinuity, and an insulating layer (in the form of a δ-function scatterer) at the interface, the transmission probability can be written in the form

$$T = \frac{4k_{\rm sc}k_{\rm nw}m_{\rm sc}m_{\rm nw}}{(k_{\rm nw}m_{\rm sc}+k_{\rm sc}m_{\rm nw})^2 + 4V_0^2 m_{\rm sc}^2 m_{\rm nw}^2/\hbar^4}; \tag{12}$$

obviously, the various scattering mechanisms are nonadditive and Matthiessen's rule is not applicable.

Slightly asymmetric junctions have essentially the same properties as the idealized symmetric ones. An NINI'N junction with insulating layers of different transparency, $T_{\rm min} \lesssim T_{\rm max}$, exhibits large imperfect resonances[23] of height $t^2(E_{\rm res}) \approx T_{\rm min}/T_{\rm max}$ instead of perfect resonances with unit transmission. Furthermore, χ^r is now a continuous function of energy; the discontinuous jumps by π are smeared (with χ^r increasing monotonuously for $T_{-L/2} < T_{L/2}$ and bounded for the opposite case with $T_{L/2} < T_{-L/2}$; note that $\chi^r + \chi^{r'} = \pi + 2\chi^t$, $\chi^{r'}$ the corresponding phase for a particle incident from the left) and $\cos\beta$ changes rapidly but smoothly between ± 1 at the resonance energies. Since all terms entering the quantization condition (7) are only weakly affected by small asymmetries, the above discussion of the electronic properties remains valid for (weakly) nonsymmetric junctions.

IV. TRANSPORT

We proceed with the investigation of the transport properties of the symmetric SINIS junctions in region I (see Fig. 6) and concentrate on the situation characterized by strong resonances with $\Gamma/\Lambda \ll 1$. Given the dependence of the quasiparticle energy ε on the phase φ, the contribution of the level to the supercurrent follows from a simple derivative, $I = (2e/\hbar)\partial_\varphi \varepsilon$ (a factor 2 has been included to account for spin degeneracy).

A. Generic case

We first consider the generic case where a level is pinned to an isolated (electronic) resonance. In this situation we can assume $t_+ \sim 1$, $t_- \propto \Gamma/\Lambda$ and $\cos(\delta\chi^t - \alpha) - r_+ r_- \cos\beta \propto \varepsilon/\Gamma + {\rm const}$ (see also Fig. 5). Within this approximation $t_+ t_- \propto \Gamma/\Lambda$ is small and linearly related to $\delta\varepsilon = \max_\varphi[\varepsilon(\varphi)] - \min_\varphi[\varepsilon(\varphi)]$ through the large slope $1/\Gamma$. We then estimate $\delta\varepsilon \propto \partial_\varphi \varepsilon \propto \Gamma^2$ and find that each level contributes a small supercurrent, of order Γ^2.

B. Degenerate resonances

The phase sensitivity of the trapped levels is dramatically increased close to degenerate resonances; see Eq. (11). However, still assuming narrow resonances with $\Gamma/\Lambda \ll 1$, the supercurrent in general remains small: within our approximation the contributions arising from a pair of nearly degenerate levels cancel each other due to the symmetry $\partial_\varphi \varepsilon^{(+)} = -\partial_\varphi \varepsilon^{(-)}$ (a more accurate analysis provides a residual contribution of order Γ^2, see Ref. 28). Furthermore, the continuous part of the spectrum again contributes with a term of

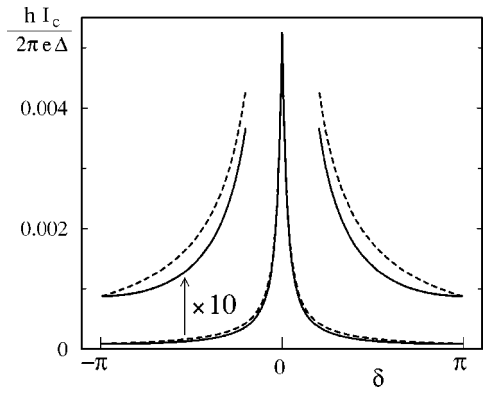

FIG. 7. Critical current versus chemical potential $\mu_{x0}=\delta\hbar/2\tau|_{\varepsilon_F}$ for a sharp resonance with $T=0.1$ and $\tau|_{\varepsilon_F}=10\hbar/\Delta$. The approximation (14) (dashed line) agrees with the exact result obtained via the Green's-function analysis at resonance and midway between resonances, $\delta=0,\pm\pi$, and provides a good estimate in between.

order Γ^2. The only situation producing a large current (of order Γ) then is realized at the special degeneracy points produced by an (electronic) resonance crossing the Fermi level, where $\hat{\varepsilon}_{\rm res}(\mu^d_{x0})\approx\check{\varepsilon}_{\rm res}(\mu^d_{x0})\approx 0$, see Fig. 6. With its energy $\varepsilon_0^{(+)}$ described by Eq. (11), this level carries a nonvanishing supercurrent of magnitude

$$I_0=\frac{2e}{\hbar}\,\frac{\Gamma^2}{16}\,\frac{\sin\varphi}{\sqrt{(\mu_{x0}-\mu^d_{x0})^2+(\Gamma/2)^2\cos^2(\varphi/2)}}. \qquad (13)$$

With one channel open, we then find that a large critical supercurrent

$$I_c(\mu_{x0})=\frac{e\Gamma}{2\hbar}\left[\sqrt{1+\left[\frac{(\mu_{x0}-\mu^d_{x0})}{\Gamma/2}\right]^2}-\frac{|\mu_{x0}-\mu^d_{x0}|}{\Gamma/2}\right] \qquad (14)$$

is realized near the special values μ^d_{x0} for the chemical potential where $\varepsilon^d_{\rm res}(\mu^d_{x0})=0$ and for $\varphi=\pi-0$. This large supercurrent flow quickly vanishes as μ_{x0} is tuned away from these degeneracy points by an energy larger than the resonance width Γ, see Fig. 7. Below, we refer to such a tunable SINIS junction as a *resonant Josephson transistor* (alternative schemes leading to a transistor effect make use of resonant electromagnetic pumping[29] or injection of quasiparticles into specific levels via multiprobe devices, see Refs. 28, 30, and 15–17). Note that the chemical potential μ_{x0} is not directly accessible but only through the gate voltage V_g, thus introducing the slope $d\mu_{x0}/dV_g$ as an additional characteristic parameter of the device. Also, we point out that a sharp transistor effect requires the temperature to be low, $k_BT<\Gamma$.

The result (14) appears to be valid in the immediate vicinity of a resonance crossing the Fermi level. However, comparing this result with the one derived from a full Green's-function analysis[31] of the long ($L\gg\xi$) SINIS junction with sharp resonances ($\Gamma/\Lambda\ll 1$), one finds that the result (14) is exact at the degeneracy points $\mu_{x0}\approx\mu^d_{x0}$ and, as it turns out, also midway in between two such degeneracies; defining the parameter $\delta=2S|_{\varepsilon_F}/\hbar\approx 2(\mu_{x0}-\mu^d_{x0})\tau|_{\varepsilon_F}/\hbar+2n\pi$, the result (14) then is exact at all multiples of π, $\delta\approx n\pi$ (here, $S|_{\varepsilon_F}$ denotes the action for an electron traversing the normal region $[-L/2+0,L/2-0]$ at the Fermi level and $\tau\equiv\partial_\varepsilon S$ is the travel time). Furthermore, in between the points $\delta=n\pi$ the deviations of Eq. (14) from the exact Green's-function result are small, see Fig. 7.

C. Josephson versus single electron transistor

Next we discuss the relation between the Josephson transistor and the superconducting single electron transistor.[32] The latter consists of two Josephson junctions separated by a superconducting grain, usually referred to as the *island*, which is capacitively (with capacitance C_g) coupled to an external gate electrode. In a more figurative terminology we might call this device a SISIS junction. While the charging energy $E_C=e^2/2C_\Sigma$ tends to fix the number of Cooper pairs on the island, the (conjugate) phase variable tends to be fixed by the Josephson coupling energy E_J of the two junctions. For the SSET, charging effects are dominant, $E_C\gg E_J$, and thus the total capacitance C_Σ of the island must be small (but still[33] $C_g\ll C_\Sigma$). Moreover we assume $E_C<\Delta$ and hence the ground state of the island contains an even number of electrons at any gate voltage. Given this layout for the device, we expect the supercurrent to be suppressed by the ''Coulomb blockade'' effect.[34] However, for specific values V_g^d of the gate voltage the energies of two even charge states differing by $2e$ become degenerate. At these ''Coulomb resonances'' the suppression of the Josephson current through the island is lifted and we find a large superflow. We can control the supercurrent by changing the gate voltage and hence the SSET constitutes a transistor device.

The above discussion shows that the SSET and the RJT are like devices, switching on as levels become degenerate; while for the SSET these levels belong to fixed charge states of the island, for the RJT these levels derive from transmission resonances. In both cases the degeneracy is lifted by the Josephson coupling $E\cos(\varphi/2)$, where the coupling constant E is related to the transmission of the NIS boundaries, see below. Furthermore, the SSET and the RJT exhibit largely the same current-voltage characteristic close to these level degeneracies,

$$I=\frac{2e}{\hbar}\,\frac{E^2}{4e\gamma}\,\frac{\sin\varphi}{\sqrt{(V_g-V_g^d)^2+[E\cos(\varphi/2)/e\gamma]^2}}, \qquad (15)$$

where the parameters E and γ have to be specified for each device. In fact, Eq. (15) yields the current through a symmetric SSET[33] if we substitute the energy parameter E by the coupling energy E_J and the dimensionless constant γ by the small ratio C_g/C_Σ. Using the Ambegaokar-Baratoff relation[35] and the Landauer formula,[36] we can reexpress the coupling energy in terms of more microscopic quantities: $E_J=NT\Delta/4$, where $N\propto k_F^2A$ denotes the number of open channels in the tunnel junction, A denotes its area, and T its transmission coefficient. On the other hand, the RJT involves

the parameters $E=\Gamma/2$ and $\gamma=\partial\mu_{x0}/\partial eV_g$. Again, the resonance width is determined by geometrical quantities: $\Gamma \approx T\Lambda/\pi$, where T is the transmittivity of the insulator layer in the triple barrier.[37] For flat inner barriers the quasiclassical method provides the simplification $\Lambda\sim 2(\mu_{x0}\varepsilon_L)^{1/2}$, with $\varepsilon_L=\hbar^2\pi^2/2mL^2$. Note that, while charging effects dominate the physics of the SSET these are much less relevant for the RJT as the latter involves an ''open wire'' rather than a ''closed island;'' the adiabatic joints to the superconducting banks provide reservoirs that effectively screen the charge transport through the wire.

From Eq. (15) we can determine the critical supercurrent I_c as a function of the gate voltage near V_g^d. Apparently, $I_c(V_g)$ defines a current peak of width $\delta V_g=E/e\gamma$ that attains its maximum $I_{\max}=eE/\hbar$ at the degeneracy point. We estimate its slope by the ratio $I_{\max}/\delta V_g=e^2\gamma/\hbar$ carrying the dimension of a conductance. For the SSET $\gamma\ll 1$ is determined through the small capacitance ratio C_g/C_Σ. The analogous quantity for the RJT is of order unity, implying that the RJT shows a more prominent slope: with $\partial\mu_{x0}/\partial eV_g=\partial_d\mu_{x0}/\partial_{eV_g}d$, and $\partial_d\mu_{x0}=2(\varepsilon_F-\mu_{x0})/d$, we have to determine the suceptibility of the channel width d with respect to the gate voltage V_g. Making use of simple electrostatic considerations one easily finds that $\partial_{\mu_{x0}}d \sim a_B/\varepsilon_F$, where a_B denotes the Bohr radius in the semiconductor material.[38,39] Hence, $\gamma\sim a_B/d$ and with a_B of order 10 nm typically we arrive at a value of order unity for the parameter γ.

Comparable energy scales $\Delta\sim\sqrt{\mu_{x0}\varepsilon_L}$ can be reached in realistic short SINIS junctions $[L\lesssim\pi(\mu_{x0}/2m)^{1/2}\hbar/\Delta]$. Furthermore, we can optimize the performance of the RJT by tuning the transparency of the insulating layers (the Dirac δ scatterers) until the resonance width Γ approaches the resonance spacing Λ; such a choice of parameters produces still isolated current peaks of maximum height. On the other hand, the maximum superflow through the SSET scales with the number N of open channels, $I_{\max}=eNT\Delta/4\hbar$, while the RJT as defined above is generically a single-channel device with a critical supercurrent $I_{\max}=eT\sqrt{\mu_{x0}\varepsilon_L}/\hbar\pi$; going over to a many-channel RJT device, resonances from individual channels superpose at *different* values for the chemical potential and hence do not add up in general.[40] Also, a smoothing of the resonance structure has been observed in the numerical results by Wendin *et al.*[6]

In summary, superconducting transistors can be designed in terms of ''charge'' (the SSET) or ''phase'' devices (the JT). In the charge device, the island is separated from the superconducting leads through insulating barriers. On the other hand, switching channels in a perfect SNS junction, one obtains a phase device with a (large) critical current $I_c=e/(\tau_0+\hbar/\Delta)$ determined by the effective time $\tau_0+\hbar/\Delta$ the charge needs to traverse the normal wire.[13] Such devices with perfect interfaces are difficult to fabricate — in reality we always have to account for a nonideal transmission $T<1$ through the SIN interfaces and we end up with a Fabry-Perot-type resonator device. Sequential tunneling through the interface barriers then reduces the supercurrent by a factor T^2 in general. However, tuning the chemical potential to a scattering resonance, the critical current of the junction remains large, $I_c\approx e\Gamma/2\hbar$ of order T — again, the critical current is given by the time $\hbar/\Gamma$ the charge spends in the junction.

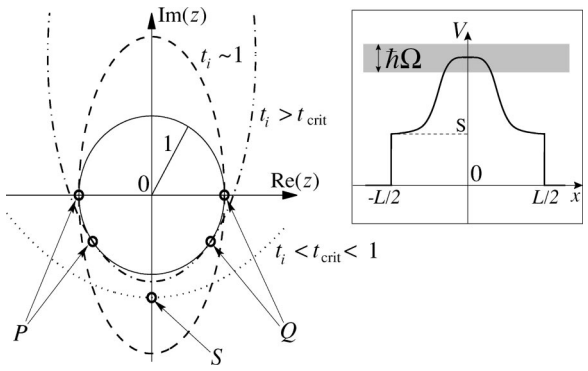

FIG. 8. Complex transmission amplitude through a smooth barrier bounded by steps. With decreasing energy E the inverse $z=1/t\exp(i\chi')$ moves counterclockwise on an ellipse, the center of which is positioned at $ir_i\sigma/t_i$ and shifts up the imaginary axis. As t_i drops below $t_{\rm crit}$ the perfect resonances at P and Q collapse at the bottom of the ellipse ($P\rightarrow S\leftarrow Q$) and transform into an imperfect (double) resonance.

A second result we wish to emphasize here concerns the fact that the critical current is carried by the lowest quasiparticle level alone. This has been demonstrated for the SNS device in Ref. 13 and above for the SINIS junction for the case of strong resonances (deviations from the single-level result are numerically (but not parametrically) larger away from weak resonances). The importance to know the dispersion of this level then provides a good *a posteriori* reason for studying the quasiparticle spectrum in such junctions. Corresponding spectroscopic experiments can be realized using multiprobe devices as proposed in the work of van Wees *et al.*[30]

ACKNOWLEDGMENTS

We thank A. Golubov, V. Shumeiko, and G. Wendin for helpful discussions and the Swiss National Foundation for financial support. The work of N.M.C. and G.B.L. was partly supported by the Russian Foundation for Basic Research under Contract No. RFFI-000216617.

APPENDIX: RESONANCE STRUCTURES IN ONE DIMENSION

We consider a one-dimensional potential landscape $V(x)$ confined to the interval $[-L/2,L/2]$. As a first example, we concentrate on a symmetric barrier consisting of a broad $[m\Omega^2=-\partial_x^2V,\ \hbar\Omega\ll V(0)]$ and smooth potential barrier, bounded by steps of height $V_S=V(L/2-0)-V(L/2+0)$ (see the inset of Fig. 8). Below we make use of the wave vectors $k_{\rm sc}=\sqrt{2mE}/\hbar$ and $k_{\rm nw}=\sqrt{2m(E-V_S)}/\hbar$ describing particles of energy E in the wire close to the boundaries. The global transmission amplitude $t\exp(i\chi')$ is most easily obtained by determining the transfer matrix[23] of the barrier between $-L/2-0$ and $L/2+0$ and we find the result

$$t\exp(i\chi^t)=\frac{t_i}{\cos(\chi^{t_i})-i\kappa\sin(\chi^{t_i})\pm ir_i\sigma}, \qquad \text{(A1)}$$

where $t_i\exp(i\chi^{t_i})$ and $r_i\exp(i\chi^{r_i})$ denote the transmission and reflection amplitudes of the inner smooth barrier. In Eq. (A1) we have introduced the definitions $\kappa=(k_{sc}/k_{nw}+k_{nw}/k_{sc})/2$ and $\sigma=(k_{sc}/k_{nw}-k_{nw}/k_{sc})/2$ containing the information about the steps. In our example, κ, σ, and t_i show a weak dependence on energy and remain almost constant, while $\exp(i\chi^{t_i})$ oscillates rapidly. The derivation of Eq. (A1) makes use of the relation $\chi^{r_i}-\chi^{t_i}=\pi/2+\pi n$, $n\in\mathbf{Z}$, which follows from the unitarity of the scattering matrix; the term $\pm ir_i\sigma$ changes sign at each perfect resonance of t_i. Since the inner barrier was assumed to be smooth, we expect t_i to exhibit no resonances at all and the term $r_i\sigma$ always carries a positive sign.

Next, we show that Eq. (A1) qualitatively reproduces the transmission amplitude shown in Fig. 2. We define the function $z=1/t\exp(i\chi^t)$, whose four arguments χ^{t_i}, κ, σ, and t_i depend on the energy. Since the inner scattering phase χ^{t_i} is the most energy sensitive argument, we minimize $|z|$ with respect to χ^{t_i} (keeping κ, σ, and t_i fixed at a given energy E). Thus we obtain the stationary phases $\chi^{t_i}_{\min}(E)$ belonging to the minima of $|z|$. Moreover, we can introduce the complex valued function $z_{\min}[E]=z[\chi^{t_i}_{\min}(E),\kappa(E),\sigma(E),t_i(E)]$, which is roughly constant when compared to $z[E]$. We can estimate the resonance energies by solving the equation $z[E_{res}]=z_{\min}[E_{res}]$ for E_{res}. Apparently, $z[E]$ describes an ellipse in the complex plane with half axes $1/t_i$ and κ/t_i. The center of this ellipse is shifted away from the origin by $ir_i\sigma/t_i$. Figure 8 illustrates the behavior of $z_{\min}$ when r_i grows from 0 to 1 in the intermediate region $E\in[V(0)-\hbar\Omega/2,\ V(0)+\hbar\Omega/2]$ [with a smooth inner barrier, r_i is strictly monotonous, $r_i\approx 0$ for $E>V(0)+\hbar\Omega/2$ and $r_i\approx 1$ for $E<V(0)-\hbar\Omega/2$]. The distance from the origin to the bottom of the ellipse (point S) is always extremal. At high energies where $1\approx t_i>1/\kappa=t_{crit}$, we observe *perfect* resonances: with $|z_{\min}|=1$ these resonances are realized at the symmetric points P and Q where the ellipse touches the unit circle, see Fig. 8. As t_i decreases, the perfect resonances approach each other (P and Q move toward S) and merge with S as $t_i\searrow t_{crit}$. At energies $E\lesssim V(0)$ ($\Rightarrow t_i<t_{crit}$) the reflection coefficient r_i drops to zero, and S becomes the closest point to the origin with $|z_{\min}|=(\kappa-\sigma r_i)/t_i>1$; the resonances then have paired up and have become *imperfect*, with a height decaying rapidly with decreasing energy E.

Physically, this resonance structure originates from the interplay of two competing transparencies. The transmission probability through the potential steps is almost constant and much smaller than the transparency of the inner barrier for $E\gg V(0)$. In this regime the particles propagate freely and are reflected by the steps alone; thus we observe perfect resonances, and the shape of the smooth inner barrier only influences the resonance spacing. On the other hand, for $E\ll V(0)$ the inner barrier behaves like a hard wall while the steps are comparatively transparent. The global transmission through the barrier bounded by the steps is suppressed by the tunneling through the classically inaccessible region. The resonances of the subsystems consisting of a step and a potential hill account for the global imperfect resonances. Note that the barrier bounded by steps generates pronounced resonances only if $V_S\gtrsim 0.7\ V(0)$.

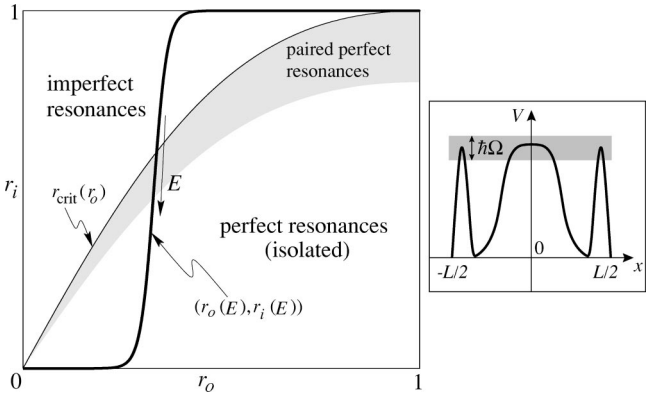

FIG. 9. The solid curve in the (r_o,r_i) plane characterizes the energy dependence of the inner and the global reflection amplitudes in a symmetric triple barrier as shown in the inset. The domains of perfect and imperfect resonances are separated by the curve $r_{crit}(r_o)$. In an narrow interval $\sim\hbar\Omega$ around $V(0)$ the reflection coefficent r_i^2 drops from 1 to 0; in this energy range r_o can be considered as a constant.

In a second step we investigate the transmission amplitude through three arbitrary symmetric potential barriers, i.e., a triple barrier, see Fig. 9. The inner barrier is again smooth, whereas the two outer barriers [characterized by the transmission and reflection amplitudes $t_o\exp(i\chi^{t_o})$ and $r_o\exp(i\chi^{r_o})$] are assumed to be equal. Thus the global transmission amplitude takes the form

$$te^{i\chi^t}=\frac{t_it_o^2e^{i(\chi^{t_i}+2\chi^{t_o})}}{1+2r_ir_oe^{i(\chi^{t_i}+\chi^{t_o})}-r_o^2e^{i2(\chi^{t_i}+\chi^{t_o})}}. \qquad \text{(A2)}$$

In order to determine the resonance structure we evaluate the extrema of the modulus of the denominator in Eq. (A2) with respect to $\chi^{t_i}+\chi^{t_o}$ (we fix t_i and t_o, which are less sensitive to changes in energy). A direct calculation yields the two extremal conditions $\cos(\chi^{t_i}+\chi^{t_o})=-r_i(1+r_o^2)/2r_o$ (I) and $\sin(\chi^{t_i}+\chi^{t_o})=0$ (II). Elementary manipulations show that the transmission amplitude exhibits *perfect* resonances in the first case. But condition I can only be satisfied as long as $r_i\leq r_{crit}(r_o)=2r_o/(1+r_o^2)$, i.e., for a reasonably transparent inner barrier (see Fig. 9). The extremal condition II requires a second distinction. Condition II(a) reads $\chi^{t_i}+\chi^{t_o}=2\pi n$, $n\in\mathbf{Z}$. The critical points of this type always belong to local minima of t. Finally, we discuss condition II(b), $\chi^{t_i}+\chi^{t_o}=\pi+2\pi n$, $n\in\mathbf{Z}$, which refers to local minima when $r_i<r_{crit}$ and characterizes *imperfect* resonances in the regime $r_i>r_{crit}$. Since the internal barrier was assumed to be smooth, the regime of perfect resonances lies at high energies $E>V(0)+\hbar\Omega/2$, where $r_i\approx 0$ and $r_o\gg r_i$. At low energies $E<V(0)-\hbar\Omega/2$, the resonances are always imper-

fect. Within the crossover region the perfect resonances attract each other pairwise and collapse to become imperfect as the energy decreases (see Fig. 2).

Other sources of resonances are discontinuities of the force $\partial_x V$ and effective mass steps. Technically they can be treated like Dirac δ scatterers and potential steps, respectively, as can be easily checked making use of the transfer-matrix formalism.

[1] For a review, see *Physics and Applications of Mesoscopic Josephson Junctions*, edited by H. Ohta and C. Ishii (The Physical Society of Japan, Kamiyama Printing, Tokyo, 1999).

[2] B.J. van Wees, H. van Houton, C.W.J. Beenakker, J.G. Williamson, L.P. Kouwenhoven, D. van der Marel, and C.T. Foxon, Phys. Rev. Lett. **60**, 848 (1988); D.A. Wharam, T.J. Thornton, R. Newbury, M. Pepper, H. Ahmed, J.E.F. Frost, D.G. Hasko, D.C. Peacock, D.A. Ritchie, and G.A.C. Jones, J. Phys. C **21**, L209 (1988).

[3] H. Takayanagi, T. Akazaki, and J. Nitta, Phys. Rev. Lett. **75**, 3533 (1995).

[4] H. van Houton, Appl. Phys. Lett. **58**, 1326 (1991).

[5] A. Chrestin, T. Matsuyama, and U. Merkt, Phys. Rev. B **49**, 498 (1994).

[6] G. Wendin and V.S. Shumeiko, Superlattices Microstruct. **20**, 569 (1996); G. Wendin, V.S. Shumeiko, P. Samuelsson, and H. Takayanagi, Jpn. J. Phys. **38**, 354 (1999); Superlattices Microstruct. **25**, 983 (1999).

[7] J.M. Krans, C.J. Muller, I.K. Yanson, Th.C.M. Govaert, R. Hesper, and J.M. van Ruitenbeek, Phys. Rev. B **48**, R14 721 (1993).

[8] C.J. Muller, J.M. van Ruitenbeek, and L.J. de Jongh, Phys. Rev. Lett. **69**, 140 (1992).

[9] E. Scheer, N. Agrait, J.C. Cuevas, A.L. Yeyati, B. Ludoph, A. Martin-Rodero, G.R. Bollinger, J.M. van Ruitenbeek, and C. Urbina, Nature (London) **394**, 154 (1998).

[10] L.I. Glazman, G.B. Lesovik, D.E. Khmel'nitskii, and R.I. Shekhter, Pis'ma Zh. Éksp. Theor. Fiz. **48**, 218 (1988) [JETP Lett. **48**, 238 (1988)].

[11] C.W.J. Beenakker, Phys. Rev. Lett. **67**, 3836 (1991).

[12] A. Furusaki, H. Takayanagi, and M. Tsukada, Phys. Rev. Lett. **67**, 132 (1991); Phys. Rev. B **45**, 10 563 (1992).

[13] N.M. Chtchelkatchev, G.B. Lesovik, and G. Blatter, Phys. Rev. B **62**, 3559 (2000).

[14] T. Akazaki, H. Takayanagi, J. Nitta, and T. Enoki, Appl. Phys. Lett. **68**, 418 (1996).

[15] A.F. Morpurgo, T.M. Klapwijk, and B.J. van Wees, Appl. Phys. Lett. **72**, 966 (1998).

[16] Th. Schraepers, J. Malindretos, K. Neurohr, S. Lachenmann, A. van der Hart, G. Crecelius, H. Hardtdegen, and H. Lüth, Appl. Phys. Lett. **73**, 2348 (1998).

[17] J.J.A. Baselmans, A.F. Morpurgo, B.J. van Wees, and T.M. Klapwijk, Nature (London) **397**, 43 (1999).

[18] A.Yu. Kasumov, R. Deblock, M. Kociak, B. Reulet, H. Bouchiat, I.I. Khodos, Yu.B. Gorbatov, V.T. Volkov, C. Journet, and M. Burghard, Science **284**, 1508 (1999).

[19] L.I. Glazman and A.V. Khaetskii, J. Phys.: Condens. Matter **1**, 5005 (1989).

[20] P.F. Bagwell, Phys. Rev. B **46**, 12 573 (1992).

[21] I.O. Kulik and A.N. Omel'yanchuk, Fiz. Nizk. Temp. **4**, 296 (1978) [Sov. J. Low Temp. Phys. **4**, 142 (1978)]; C. Ishii, Prog. Theor. Phys. **44**, 1525 (1970).

[22] A.F. Andreev, Zh. Éksp. Teor. Fiz. **46**, 1823 (1964) [Sov. Phys. JETP **19**, 1228 (1964)].

[23] B. Ricco and M.Ya. Azbel, Phys. Rev. B **29**, 1970 (1984).

[24] Note that in Ref. 13 basis states have been chosen where the phases vanish at the center of the junction.

[25] G.A. Gogadze and A.M. Kosevich, Fiz. Nizk. Temp. **24**, 716 (1998) [Sov. J. Low Temp. Phys. **24**, 540 (1998)].

[26] It is convenient to separate the effects of normal and Andreev scattering through a thin normal metallic layer of width $\delta \to 0$.

[27] Note that in our convention Γ is twice as large as in Ref. 6.

[28] G. Wendin and V.S. Shumeiko, Phys. Rev. B **53**, R6006 (1996).

[29] V.S. Shumeiko, G. Wendin, and E.N. Bratus, Phys. Rev. B **48**, 13 129 (1993).

[30] B.J. van Wees, K.-M.H. Lenssen, and C.J.P.M. Harmans, Phys. Rev. B **44**, 470 (1991).

[31] N.M. Chtchelkatchev (unpublished).

[32] P. Joyez, P. Lafarge, A. Filipe, D. Esteve, and M.H. Devoret, Phys. Rev. Lett. **72**, 2458 (1994).

[33] M. Tinkham, *Introduction to Superconductivity* (McGraw-Hill, New York, 1996).

[34] D.V. Averin and K.K. Likharev, in *Mesoscopic Phenomena in Solids*, edited by B.L. Altshuler, P.A. Lee, and R.A. Webb (North-Holland, Amsterdam, 1991), p. 213.

[35] V. Ambegaokar and A. Baratoff, Phys. Rev. Lett. **10**, 486 (1963).

[36] M. Büttiker, Y. Imry, R.H. Landauer, and S. Pinhas, Phys. Rev. B **31**, 6207 (1985).

[37] The term ''triple barrier'' is defined in Appendix A.

[38] L.I. Glazman and A.V. Khaetskii, Europhys. Lett. **9**, 263 (1989).

[39] I.A. Larkin and J.H. Davies, Phys. Rev. B **52**, R5535 (1995).

[40] N.M. Chtchelkatchev, Pis'ma Zh. Eksp. Teor. Fiz. **71**, 738 (2000).